


















RESEARCH ARTICLE OPEN ACCESS

ALX/FPR2 Contributes to Serum Amyloid A-Induced Lung Neutrophil Recruitment Following Acute Ozone Exposure

Michael J. Yaeger¹  | Tyson Ngatikaura¹  | Natali Zecchino¹  | Katelyn Dunigan-Russell¹  | Hannah B. Lovins¹  |
 Evangeline Schott¹  | Grace Hutton¹  | Brett Saunders¹  | Yan Lin²  | Junfeng (Jim) Zhang²  |
 Samuel J. Cochran¹  | Rafia Virk³  | R. Ian Cumming⁴  | Salik Hussain⁴  | Robert M. Tighe⁵  |
 Saame Raza Shaikh³  | Kimberly M. Gowdy¹ 

¹Department of Internal Medicine, Ohio State University Wexner Medical Center, Columbus, Ohio, USA | ²Nicholas School of the Environment, Duke University, Durham, North Carolina, USA | ³Department of Nutrition, Gillings School of Global Public Health and School of Medicine, University of North Carolina at Chapel Hill, Chapel Hill, North Carolina, USA | ⁴Department of Physiology, Pharmacology & Toxicology, West Virginia University, Morgantown, West Virginia, USA | ⁵Department of Medicine, Duke University, Durham, North Carolina, USA

Correspondence: Michael J. Yaeger (michael.yaeger@osumc.edu) | Kimberly M. Gowdy (kymberly.gowdy@osumc.edu)

Received: 15 November 2024 | **Revised:** 14 March 2025 | **Accepted:** 11 April 2025

Funding: This work was supported by Foundation for the National Institutes of Health (FNIH) (S10RR027926, S10OD032292, F31ES036102-02, P30DK056350, R01ES031378, R01ES034350, and R01ES031253).

Keywords: ALX/FPR2 | lung | neutrophil | ozone | serum amyloid A

ABSTRACT

Ozone (O₃) is a toxic air pollutant that causes pulmonary inflammation, neutrophil recruitment, and lung injury. Part of the inflammatory response to O₃ includes altered expression of formyl peptide receptor 2 (ALX/FPR2), a G protein-coupled receptor expressed primarily in immune cells. ALX/FPR2 is considered either anti-inflammatory/proresolving or proinflammatory depending on its ligands, which include lipoxin A4 or serum amyloid A (SAA). While the anti-inflammatory/proresolving lipoxin A4 ligand has been well studied, there remains a significant knowledge gap in the interaction between proinflammatory SAA and ALX/FPR2. To date, SAA has been shown to increase neutrophil recruitment through ALX/FPR2 and is increased systemically after O₃ exposure. However, it is unclear if pulmonary SAA signals through ALX/FPR2 during the O₃-induced inflammatory response. We hypothesized that ALX/FPR2-SAA signaling is required to initiate neutrophil recruitment to the lungs following O₃ exposure. To test this hypothesis, ALX/FPR2 wild type (FPR2^{+/+}) or knockout (FPR2^{-/-}) mice were exposed to filtered air (FA) or 1 ppm O₃ for 3 h. Pulmonary inflammation was assessed 6, 24, and 48 h following O₃ exposure. FPR2^{-/-} mice exhibited impaired neutrophil recruitment at 6 and 24 h after O₃ exposure. In addition, FPR2^{-/-} mouse pulmonary SAA expression was significantly increased after O₃ exposure compared to FPR2^{+/+} mice. FPR2^{+/+} mice dosed with SAA via oropharyngeal aspiration had increased pulmonary neutrophils, while neutrophils were not increased in FPR2^{-/-} mice. Taken together, these data indicate that ALX/FPR2 may contribute to SAA-induced pulmonary neutrophilia following O₃ exposure.

1 | Introduction

Air pollution is the fourth highest risk factor for death and was attributed to more than 6.67 million deaths globally in 2019 [1]. Ozone (O₃) is a major contributor to the adverse health effects from air pollution. This is in part because it induces lung

inflammation/injury and increases the incidence and exacerbation of chronic lung diseases [2, 3]. Furthermore, tropospheric levels of O₃ have increased over the last several years, which has led to increased acute O₃ exposures [4, 5]. This is of concern because acute O₃ exposure is correlated with increased hospitalizations and deaths, particularly in people with preexisting

This is an open access article under the terms of the [Creative Commons Attribution](https://creativecommons.org/licenses/by/4.0/) License, which permits use, distribution and reproduction in any medium, provided the original work is properly cited.

© 2025 The Author(s). *The FASEB Journal* published by Wiley Periodicals LLC on behalf of Federation of American Societies for Experimental Biology.

cardiopulmonary diseases [6–9]. Therefore, it is important to define the biological mechanisms by which O₃ contributes to lung inflammation and injury to better identify how to mitigate detrimental health effects from O₃ exposure.

O₃ causes lung injury partly through activating the inflammatory response [10]. When inhaled, O₃ does not directly interact with cells, but rather interacts with the airway surface liquid where it oxidizes phospholipids, proteins, mucins, and cholesterol [2]. These O₃-induced modifications generate damage associated molecular patterns (DAMPs), molecular signals which are then detected by pattern recognition receptors such as toll-like receptor 4 (TLR4). Signaling through TLR4 leads to downstream activation of transcription factors such as nuclear transcription factor- κ B (NF- κ B) which transcribe proinflammatory cytokines and chemokines [2, 11–13]. These cytokines and chemokines activate the acute phase response, including production of serum amyloid A (SAA), which then recruits innate immune cells (i.e., neutrophils) to the lungs [14–16].

We previously published that O₃ exposure decreases pulmonary expression of the SAA receptor, ALX/FPR2 [17]. ALX/FPR2 is a 7-pass transmembrane G protein-coupled receptor implicated in pulmonary diseases such as asthma [18, 19], pneumosepsis [20], and fibrosis [21]. ALX/FPR2 is expressed primarily on leukocytes and airway epithelial cells and has many ligands that impart differing biological responses [22]. For example, in addition to binding with the proinflammatory SAA, anti-inflammatory/proresolving lipid metabolites termed specialized proresolving mediators (SPMs)—such as lipoxin A₄ (LXA₄) and resolvin D1 (RvD₁)—signal through ALX/FPR2 [23–25]. The biased agonism of ALX/FPR2 is still unclear; however, it has been suggested these ligand-dependent effects are influenced by ALX/FPR2 heterodimerizing with proinflammatory FPR1 or FPR3, or homodimerizing to detect anti-inflammatory ligands [26]. Because of ALX/FPR2's wide range of bioactivity, it is important to consider both its anti-inflammatory and proinflammatory aspects. Presently, it is unclear if SAA signals through ALX/FPR2 during the pulmonary inflammatory response to O₃. Therefore, we hypothesized that ALX/FPR2-SAA signaling is required to initiate neutrophil recruitment in the lungs following O₃ exposure by detecting SAA. In this study, loss of ALX/FPR2 reduced neutrophil recruitment to the lung following O₃ exposure. Neutrophil recruiting chemokines were not disrupted in FPR2^{−/−} mice and the SPM response was unaltered. However, FPR2^{−/−} mice had significantly increased SAA expression in the lung after O₃ exposure. Exogenous SAA administration caused significant neutrophil recruitment to the lungs only in FPR2^{+/+} mice, but not FPR2^{−/−} mice. Overall, these data indicate that ALX/FPR2 is required for SAA to recruit neutrophils to the lung following O₃ exposure.

2 | Materials and Methods

2.1 | Animals

Male ALX/FPR2 wild type (FPR2^{+/+}) and ALX/FPR2 knock-out (FPR2^{−/−}) mice, 8–12 weeks old, were used for this study. Given the known role of sex as well as the estrous cycle on the O₃-induced inflammatory responses, only males were used [27].

These mice were generated by the UNC Chapel Hill Animal Models Core using CRISPR-Cas9 targeting the 5' and 3' flanking regions of ALX/FPR2 exon 2 as previously described [28]. Mice were bred in-house for experiments, and genotypes were confirmed via PCR and gel electrophoresis. All experiments were performed in accordance with the Animal Welfare Act and the U.S. Public Health Service Policy on Humane Care and Use of Laboratory Animals after review by the Animal Care and Use Committees of The Ohio State University.

2.2 | Murine In Vivo Exposure

FPR2^{+/+} and FPR2^{−/−} mice were exposed inside a modified metal Hinner's chamber to filtered air (FA) or 1 ppm of O₃ for 3 h. This exposure mimics what a human would experience on an 'O₃ action day' [29, 30]. O₃ was generated and measured as previously described and temperature and humidity were monitored continuously [17]. Mice were euthanized 6, 24, or 48 h after exposure with an intraperitoneal injection of a ketamine (100 mg/kg) and xylazine (10 mg/kg) mixture as previously described [31]. For CXCL1 experiments, FPR2^{+/+} and FPR2^{−/−} mice were anesthetized with isoflurane and dosed with 0.5 μ g/mouse via oropharyngeal aspiration (OA) in 50 μ L of CXCL1 (R&D Systems, MN, USA) or vehicle control (PBS). In additional experiments, FPR2^{+/+} and FPR2^{−/−} mice were anesthetized with isoflurane and dosed with 10 μ g/mouse via OA in 50 μ L of recombinant mouse SAA₁ (<0.1 EU/ μ g; R&D Systems, MN, USA), recombinant mouse SAA₃ (<1 EU/ μ g; Cusabio, TX, USA), or vehicle control (PBS). Mice were then euthanized 4 h after dosing with CXCL1 as previously described [32], and 24 h after dosing with SAA.

2.3 | Bronchoalveolar Lavage Fluid (BALF) Collection and Analysis

The right lung was lavaged with three separate volumes of 26.25 mL/kg of PBS as previously described [27]. BALF was then centrifuged at 460 \times g for 6 min at 4°C. Total protein was measured in BALF supernatant using the bicinchoninic acid (BCA) Protein Assay Kit (Thermo Fisher Scientific, MA, USA). Cellular differentials of cells collected in BALF were performed as previously described [27]. Additional BALF supernatant was concentrated with Amicon Ultra Centrifugal Filters (MilliporeSigma, MA, USA) before measuring cytokines and chemokines by MESO QuickPlex analysis (Mesoscale Discovery, MD, USA) per the manufacturer's instructions. Cytokines and chemokines measured in BALF supernatant included: C-C motif ligand 2 (CCL2), C-X-C motif ligand 2 (CXCL2), C-X-C motif ligand 1 (CXCL1), interleukin-6 (IL-6), interleukin-1 β (IL-1 β), and tumor necrosis factor- α (TNF- α).

2.4 | Plasma SAA ELISA

Blood was collected by cardiac puncture with a 25 G needle and transferred to a dipotassium ethylenediaminetetraacetic acid (K₂EDTA) plasma tube (BD Biosciences, NJ, USA). The collected blood was centrifuged at 200 \times g for 10 min at 4°C. Plasma supernatant was then collected and stored at −80°C until analysis.

TABLE 1 | Flow cytometry antibodies.

Antibody	Fluorophore	Dilution	Clone	Vendor
Blood				
CD45	APC/Cy7	1:100	30-F11	BioLegend
CD11b	BV711	1:100	M1/70	BioLegend
Ly6g	BV421	1:100	1A8	BioLegend
BALF				
CD45	APC/Cy7	1:100	30-F11	BioLegend
Ly6g	APC	1:100	S19019G	BioLegend
Lung tissue				
CD206	FITC	1:400	C068C2	BioLegend
SiglecF	PE/CF594	1:1500	E50-2440	BD Biosciences
Ly6G	AF700	1:200	1A8	BioLegend
CD11b	APC/Cy7	1:150	M1/70	BioLegend
CD64	BV421	1:200	X54-5/7.1	BioLegend
CD45	BV605	1:500	30-F11	BioLegend
IA/IE	BV650	1:1500	M5/114.15.2	BioLegend
CD24	BV711	1:800	M1/69	BioLegend
CD11c	BV785	1:150	N418	BioLegend
Zombie UV		1:1000		BioLegend

SAA concentrations in plasma were analyzed by ELISA using a mouse SAA quantikine ELISA kit (R&D Systems, MN, USA) per the manufacturer's instructions.

2.5 | MPO Assay

Unperfused left lung lobes were collected immediately following euthanasia and snap frozen in liquid nitrogen. Frozen lung tissue was then homogenized via bead homogenization in 200 μ L of assay buffer for MPO activity (Abcam, Cambridge, United Kingdom). Lung tissue homogenate was then centrifuged at 13000 \times g for 10 min, and the supernatant was collected. BCA protein assay (Thermo Fisher Scientific, MA, USA) was performed on the homogenate supernatant, and then the MPO assay was performed on the supernatant per the manufacturer's instructions.

2.6 | RNA Isolation and Quantitative Polymerase Chain Reaction (qPCR)

Left lung lobes were collected immediately after euthanasia, sealed in a cryotube, and snap frozen in liquid nitrogen until RNA isolation. Lung tissue was homogenized, and RNA was isolated using a Qiagen RNeasy Mini Kit (Fisher Scientific, NH, USA) according to the manufacturer's instruction. RNA was quantified using a NanoDrop 1000 Spectrophotometer (Thermo Fisher Scientific, MA, USA) or SpectraMax iD3 Multi-Mode Microplate Reader (VWR, PA, USA). cDNA was synthesized

from RNA using the RevertAid First Strand cDNA Synthesis Kit per the manufacturer's instructions (Thermo Fisher, MA, USA). Real-time qPCR was performed with Taqman PCR Mix (Applied Biosystems, MA, USA) in the HT7900 ABI sequence Detection System (Applied Biosystems, MA, USA) using pre-designed primers (Applied Biosystems, MA, USA). Fold changes in expression of mRNA were calculated using Ct values and the $2^{-\Delta\Delta C_t}$ method. Samples were normalized to 18S as previously described [33]. Taqman primers used for this research were 18S (Mm03928990_g1), SAA₁ (Mm00656927_g1), SAA₃ (Mm00441203_m1), and ALX/FPR2 (Mm00484464_s1) (Thermo Fisher Scientific, MA, USA).

2.7 | Flow Cytometry

Blood, BALF, and lung tissue were collected for extracellular staining and flow cytometry analysis. Blood was collected by cardiac puncture with a 25 G needle into a K₂EDTA tube. Then, 50 μ L of blood was mixed with Fc blocking solution (antimouse CD16/32; clone 93; BioLegend, CA, USA) for 15 min, followed by incubation with an antibody mix solution for 20–30 min (antibodies listed in Table 1). Then, red blood cells (RBCs) were lysed with 1X BD's RBC lysing solution (BD Biosciences, NJ, USA), and the remaining cells were suspended in FACS buffer (PBS, 3% FBS, 10 mM EDTA, 10 mM HEPES). For BALF flow cytometry, the whole lung was lavaged with three separate volumes of 35 mL/kg of HBSS. BALF was then centrifuged at 460 \times g for 6 min at 4°C, the supernatant was aspirated, and RBCs were lysed with ACK RBC lysis buffer (0.17M NH₄Cl, 10 mM

KHCO₃, 250 μM EDTA in diH₂O, pH 7.5) for 1 min before ending the lysis reaction with 4 mL of HBSS. The cells were then centrifuged at 460×g for 6 min at 4°C, the supernatant was aspirated, the cells were resuspended in 1 mL HBSS +1% FBS, and cellular counts were performed on a hemacytometer. The cells were then stained with 10 mM 2',7'-dichlorodihydrofluorescein diacetate (H2DCFDA; Thermo Fisher Scientific, MA, USA)—which converts to 2',7'-dichlorofluorescein (DCF) upon oxidation—for 20 min, followed by blocking with Fc blocking solution (antimouse CD16/32; clone 93; BioLegend, CA, USA), followed by staining with antibody mix solution for 30 min. Flow cytometry on blood and BALF samples was performed on the Cytex Northern Lights (Cytex Biosciences, CA, USA) spectral flow cytometer, and analysis was performed in FlowJo software (BD Life Sciences, NJ, USA). For lung tissue flow cytometry, lungs were perfused by injecting up to 10 mL of PBS into the right atrium/ventricle using a 25 G needle. The lungs were then instilled through the trachea with 2–3 mL digest buffer (5 mg/mL collagenase +0.4 mg/mL DNase +5% FBS). Filled lungs were excised and placed in a 50 mL tube with 5–10 mL additional digest buffer and incubated in a hot water bath at 37°C for 30 min, with vortexing every 8–10 min. The enzymatic reaction was stopped by filling the rest of the tube with PBS, and digested tissue was filtered through a 70 μm cell strainer. The single cell suspension was then centrifuged at 250×g for 6–8 min at 4°C, and RBCs were lysed with 3 mL of ACK RBC lysis buffer for 3–5 min. The single cell suspension was then pelleted and resuspended for cell counts. Approximately 10⁷ cells were stained with zombie UV (1:500; BioLegend) for 15–20 min, washed, and then fixed with 1.5% paraformaldehyde and stored at 4°C. For antibody staining, cells were incubated with Fc blocking solution (BioLegend, CA, USA) for 7–10 min and then stained with the antibody mix solution for 30 min (antibodies listed in Table 1) as previously described by Yu et al. [34]. Flow cytometry was performed on an LSR Fortessa X-20, and data analysis was performed in FlowJo.

2.8 | Liquid Chromatography-Mass Spectrometry

All standards and internal standards used for reverse phase high performance liquid chromatography (HPLC) tandem mass spectrometry (LC-MS/MS) analysis of lipid mediators were purchased from Cayman Chemical (Ann Arbor, Michigan). All HPLC solvents and extraction solvents were HPLC grade. Left lung tissue was homogenized, and lipid mediators were isolated as previously described [27]. The samples were analyzed immediately or frozen at –70°C until analysis. Isolated lipid metabolites were analyzed by LC-MS/MS as previously described [17]. Briefly, the Agilent 6490 triple quadrupole mass spectrometer in negative ionization mode was used to detect lipid mediators. The Agilent Masshunter Quantitative Analysis software was used to calculate calibration curves, which were then used to calculate pg/mg of wet tissue. All standards were purchased from Cayman Chemical. All nondetectable samples were assigned a value of zero for statistical analysis.

2.9 | Statistical Analysis

Data points were pooled from two separate experiments and are expressed as mean ± standard error of the mean (SEM).

Data were analyzed using two-way ANOVA followed by Šidák's multiple comparisons test post hoc to correct for multiple comparisons. A value of $p < 0.05$ was considered significant. For Figure 5A–F, lipidomic data were normalized by min-max scaling following the equation: $x_{scaled} = \frac{x - x_{min}}{x_{max} - x_{min}}$ [35]. These data were normalized to better assess changes in the overall lipidome without individual high-concentration lipids (e.g., 12-HETE, 14-HDoHE, 12-HEPE) disproportionately influencing the results.

3 | Results

3.1 | ALX/FPR2 Expression in the Lung is Altered by O₃ Exposure

To first assess how ALX/FPR2 changes over the course of the inflammatory response to O₃ exposure, *Fpr2* gene expression in lung tissue was measured at 6, 24, and 48 h after exposure (Figure 1). At 6 h, *Fpr2* expression was increased in O₃-exposed mice compared to FA. Then, at 24 h, *Fpr2* was not statistically altered in O₃-exposed mice compared to FA. Finally, at 48 h, *Fpr2* was significantly decreased in O₃-exposed mice compared to FA. Overall, these findings show that *Fpr2* gene expression in lung tissue is altered by O₃ exposure in a time-dependent manner.

3.2 | ALX/FPR2 Contributes to the Initiation of O₃-Induced Pulmonary Inflammation

Given that *Fpr2* expression in the lung was changed following O₃ exposure, we sought to evaluate the impact of ALX/FPR2 on immune cell recruitment and lung injury after O₃ exposure. FPR2^{–/–} and FPR2^{+/+} mice were exposed to whole-body FA or 1 ppm O₃ for 3 h and necropsied 6, 24, or 48 h following exposure. At 6 h following O₃ exposure, airspace neutrophils were increased in FPR2^{+/+} but not in FPR2^{–/–} mice and were significantly decreased in FPR2^{–/–} compared to FPR2^{+/+} mice (Figure 2A). Then 24 h following O₃ exposure, airspace neutrophilia continued to be increased compared to FA groups in FPR2^{+/+} mice, but not in FPR2^{–/–} mice (Figure 2A). At 48 h following O₃ exposure, BALF neutrophils were increased in both FPR2^{+/+} and FPR2^{–/–} mice with no differences between genotypes (Figure 2A). O₃ did not alter numbers of airspace

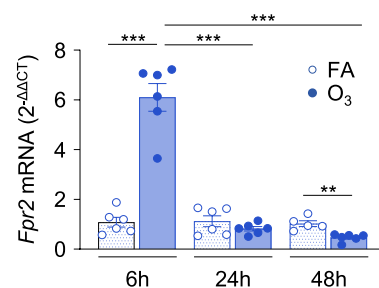


FIGURE 1 | Lung ALX/FPR2 expression in the lung is altered by ozone exposure. ALX/FPR2 wild type (FPR2^{+/+}) male mice 8–12 weeks old were exposed to filtered air (FA) or 1 ppm ozone (O₃) for 3 h, and necropsied 6, 24, or 48 h after the start of the exposure. Lung tissue was collected for real-time PCR analysis. ** $p < 0.01$, *** $p < 0.001$, $n = 5–6$ /group.

macrophages at 6 or 24h; however, O₃ significantly increased BALF macrophages in FPR2^{-/-} mice at 48h after exposure (Figure 2B). O₃ exposure increased microvascular and alveolar epithelial permeability, as measured via BALF protein, at

all timepoints post exposure. At 6 and 24h following O₃, BALF protein was not different between FPR2^{+/+} and FPR2^{-/-} mice (Figure 2C). At 48h post exposure, O₃-exposed FPR2^{-/-} mice had statistically increased BALF protein compared to FPR2^{+/+}

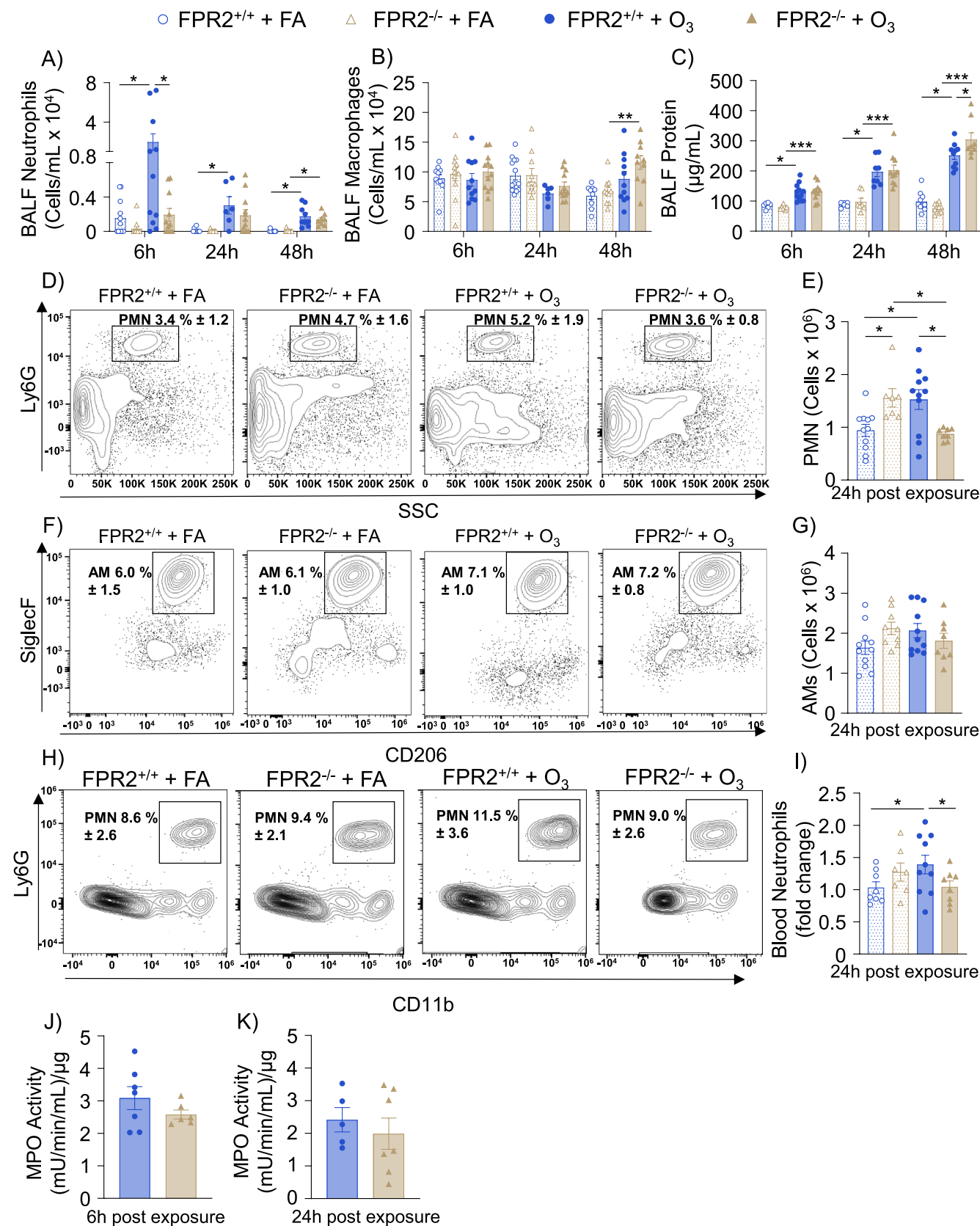


FIGURE 2 | Legend on next page.

FIGURE 2 | ALX/FPR2 contributes to the initiation of ozone-induced pulmonary inflammation. ALX/FPR2 wild type (FPR2^{+/+}) or ALX/FPR2 knockout (FPR2^{-/-}) male mice 8–12 weeks old were exposed to filtered air (FA) or 1 ppm ozone (O₃) for 3 h and necropsied 6, 24, or 48 h after the start of the exposure. (A) Bronchoalveolar lavage fluid (BALF) was collected for cellular differentials of neutrophils, and (B) macrophages, and for (C) protein analysis. Lung tissue was collected for flow cytometry analysis of (D, E) neutrophils, and (F, G) alveolar macrophages (AMs). (H, I) Blood was collected for flow cytometry analysis of neutrophils. Lung tissue was collected for MPO activity analysis at (J) 6 h and (K) 24 h following O₃ exposure. MPO activity is reported in milliunits (mU) per minute of enzymatic reaction per milliliter (mL) of reaction volume per microgram (μg) of total protein in the reaction well. **p* < 0.05, ****p* < 0.001, *n* = 6–13/group.

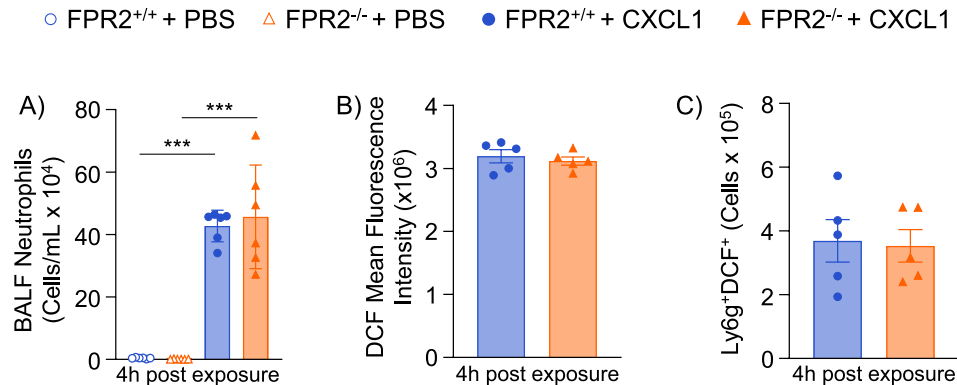


FIGURE 3 | FPR2^{-/-} neutrophils retain chemotactic and reactive oxygen species producing function. ALX/FPR2 wild type (FPR2^{+/+}) or ALX/FPR2 knockout (FPR2^{-/-}) male mice 8–12 weeks old were dosed by oropharyngeal aspiration (OA) with PBS or 0.5 μg/mouse CXCL1 and then necropsied 4 h after exposure. Bronchoalveolar lavage fluid (BALF) was collected for (A) cellular differentials of neutrophils, and (B/C) flow cytometry analysis of reactive oxygen species using a 2',7'-dichlorofluorescein (DCF) dye. ****p* < 0.001, *n* = 5–6/group.

mice (Figure 2C). These findings suggest that ALX/FPR2 contributes to increased airspace neutrophils during the initiation of inflammation as well as protects against lung injury following O₃ exposure at later timepoints.

3.3 | ALX/FPR2 Facilitates O₃-Induced Pulmonary Neutrophil Recruitment

Reduced airspace neutrophilia in FPR2^{-/-} mice could result from impaired neutrophil trafficking from the interstitium to the airspace. To investigate this, flow cytometry was performed on perfused and digested lung tissue to evaluate whole lung neutrophilia. Flow cytometry indicated that neutrophils were increased in the lung tissue of FPR2^{-/-} mice 24 h following FA exposure when compared to FPR2^{+/+} mice (Figure 2D,E). 24 h following O₃ exposure, neutrophils were increased in FPR2^{+/+} mice and were significantly decreased in FPR2^{-/-} mice compared to FPR2^{+/+} mice (Figure 2D,E). Alveolar macrophages were also evaluated by flow cytometry, which were not altered by exposure and/or genotype (Figure 2F,G). Since neutrophils were decreased in both the airspace and the whole lung, these data suggest that ALX/FPR2 influences neutrophil recruitment to the lung. To understand whether altered pulmonary neutrophil migration results from reduced systemic levels, blood neutrophils were measured by flow cytometry. O₃ significantly increased neutrophilia in the blood of FPR2^{+/+} mice but did not alter neutrophils in the blood of FPR2^{-/-} mice (Figure 2H,I). Moreover, among O₃-exposed animals, blood neutrophils were significantly decreased in FPR2^{-/-} mice compared to FPR2^{+/+} mice (Figure 2E,F). This suggests reduced circulating neutrophil

levels, perhaps due to reduced chemotaxis from the bone marrow. Lung tissue myeloperoxidase (MPO) was also measured to determine if loss of ALX/FPR2 disrupts neutrophil function in addition to chemotaxis following O₃ exposure. At both 6 and 24 h following O₃ exposure, MPO was not significantly altered between FPR2^{+/+} and FPR2^{-/-} mice (Figure 2J,K). Therefore, the effect of ALX/FPR2 on neutrophils appears to be limited to their recruitment following O₃ exposure.

3.4 | FPR2^{-/-} Neutrophils Retain Chemotactic and Reactive Oxygen Species Producing Functions

To then identify if neutrophils lacking ALX/FPR2 had reduced chemotactic responsiveness, mice were dosed by OA with CXCL1, a neutrophil-recruiting chemokine. Following CXCL1 dosing, both FPR2^{+/+} and FPR2^{-/-} mice had increased airspace neutrophilia with no differences between genotypes (Figure 3A). This suggests that FPR2^{-/-} neutrophils can still be chemotactically recruited to the lungs and therefore the effect of ALX/FPR2 on pulmonary neutrophil chemotactic signaling is indirect. To identify if the loss of ALX/FPR2 disrupts neutrophil function, neutrophils from the BALF were also evaluated for reactive oxygen species (ROS), using the 2',7'-dichlorodihydrofluorescein diacetate (H₂DCFDA) dye that converts to the highly fluorescent 2',7'-dichlorofluorescein (DCF) upon oxidation. Neutrophils from FPR2^{-/-} mice had the same mean fluorescence intensity for DCF, as well as the same number of Ly6G⁺DCF⁺ cells as FPR2^{+/+} mice when stimulated with CXCL1 by OA (Figure 3B,C). This indicates FPR2^{-/-} neutrophils retain their ROS production function.

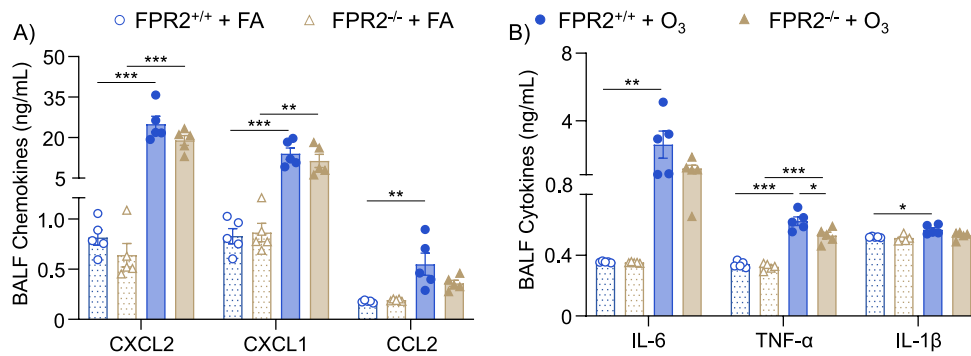


FIGURE 4 | Initiation of inflammatory signaling is not disrupted with loss of ALX/FPR2 following ozone exposure. ALX/FPR2 wild type (FPR2^{+/+}) or ALX/FPR2 knockout (FPR2^{-/-}) male mice 8–12 weeks old were exposed to filtered air (FA) or 1 ppm ozone (O₃) for 3 h and necropsied 6 h after the start of the exposure. Bronchoalveolar lavage fluid (BALF) was collected for mesoscale analysis of (A) chemokines and (B) cytokines. **p* < 0.05, ***p* < 0.01, ****p* < 0.001, *n* = 5/group.

3.5 | Inflammatory Signaling Is Not Disrupted With Loss of ALX/FPR2 Following O₃ Exposure

To define potential reasons why neutrophils are not effectively recruited to the lungs in FPR2^{-/-} mice after O₃ exposure, airspace cytokines and chemokines were measured in the BALF. CXCL1 and CXCL2 (neutrophil recruiting chemokines) were increased in both FPR2^{+/+} and FPR2^{-/-} mice with no differences between genotypes 6 h after O₃ exposure (Figure 4A). CCL2 (monocyte recruiting chemokine) was statistically increased in FPR2^{+/+} mice but not in FPR2^{-/-} mice after O₃ exposure (Figure 4A). IL-6 and IL-1β were increased only in FPR2^{+/+} mice after O₃ exposure (Figure 4B). TNF-α was also increased in both FPR2^{+/+} and FPR2^{-/-} mice but decreased in FPR2^{-/-} mice compared to FPR2^{+/+} mice after O₃ exposure (Figure 4B). Thus, loss of ALX/FPR2 influences the production of select proinflammatory cytokines and chemokines but not neutrophil-recruiting chemokines. Given that neutrophil-recruiting chemokines were unaffected, this suggests a role for other O₃-induced soluble mediators.

3.6 | Loss of ALX/FPR2 Does Not Influence Pulmonary Oxylipins

Neutrophil recruitment can also be influenced by oxylipins derived from n-6 (typically proinflammatory eicosanoids) and n-3 (typically anti-inflammatory/proresolving SPMs) polyunsaturated fatty acids [36–38]. Furthermore, ALX/FPR2 is a known receptor for SPMs LXA4 and RvD1. Therefore, oxylipins were measured in lung tissue by targeted LC-MS/MS to determine whether they were altered by the loss of ALX/FPR2, which may have led to changes in neutrophil recruitment following O₃ exposure. Separating oxylipins by parent fatty acids, arachidonic acid (AA; 20:4 n-6), docosahexaenoic acid (DHA; 22:6 n-3), and eicosapentaenoic acid (EPA; 20:5 n-3) derived oxylipins were not statistically altered by exposure or genotype. However, DHA-derived oxylipins appeared to nonstatistically increase after O₃ exposure, particularly in FPR2^{-/-} mice (Figure 5A–F). Furthermore, there were no changes in the ALX/FPR2 ligand, LXA4 (Figure 5G), or other SPMs such as RvD6 (Figure 5H) or MaR1 (Figure 5I) 24 h after FA or O₃ exposure. The other SPM ligand for ALX/FPR2, RvD1, was below the limit of detection and unable to be quantified. All detected oxylipins are presented in Table S1. Overall, the loss of

ALX/FPR2 signaling does not likely exert an effect on neutrophilia by disrupting oxylipin concentrations.

3.7 | SAA Expression and Production Are Disrupted With Loss of ALX/FPR2

With no changes in neutrophil recruiting chemokines or proresolving SPMs, SAA—a pro-inflammatory ligand for ALX/FPR2—was investigated. There are three members of the SAA family expressed in mice that function in acute phase responses (SAA_{1–3}), and a fourth SAA, SAA₄, is constitutively expressed. SAA₁ and SAA₂ are homologous and mostly produced in the liver but can also be produced extrahepatically, while SAA₃ is mostly expressed extrahepatically [39, 40]. O₃ exposure induced pulmonary *Saa*₁, *Saa*₂, *Saa*₃, and *Saa*₄ expression in FPR2^{+/+} mice (Figure 6A–D). In FPR2^{-/-} mice, *Saa*₁ and *Saa*₃ were significantly increased, and *Saa*₂ was not different compared to FPR2^{+/+} mice after O₃ exposure (Figure 6A–C). *Saa*₄ was not increased in FPR2^{-/-} mice after O₃ exposure (Figure 6D). Plasma concentrations of total SAA were also measured by ELISA. Plasma SAA was significantly increased in FA exposed FPR2^{-/-} mice compared to FA exposed FPR2^{+/+} mice (Figure 6E). FPR2^{+/+} mice had increased plasma SAA after O₃ exposure compared to FA, while SAA concentrations remained elevated in FPR2^{-/-} mice, near equivalent to concentrations in FPR2^{+/+} mice, after O₃ exposure (Figure 6E). Thus, pulmonary and systemic SAA regulation is disrupted by loss of ALX/FPR2 before and after O₃ exposure.

3.8 | SAA₁ Contributes to Neutrophil Recruitment Through ALX/FPR2

In this study, changes in pulmonary and systemic SAA correlated with inhibited pulmonary neutrophil recruitment following O₃ exposure. Because SAA-ALX/FPR2 signaling leads to increased neutrophil recruitment, the loss of ALX/FPR2 may result in reduced signaling from SAA and subsequently reduced airspace neutrophil recruitment following O₃ exposure. To test this, mice were dosed via OA with recombinant mouse SAA₁ or SAA₃. FPR2^{+/+} mice dosed with SAA₁ had increased BALF neutrophils whereas FPR2^{-/-} mice dosed with SAA₁ did not have increased BALF neutrophils (Figure 7A). Both FPR2^{+/+} and

○ FPR2^{+/+} + FA △ FPR2^{-/-} + FA ● FPR2^{+/+} + O₃ ▲ FPR2^{-/-} + O₃

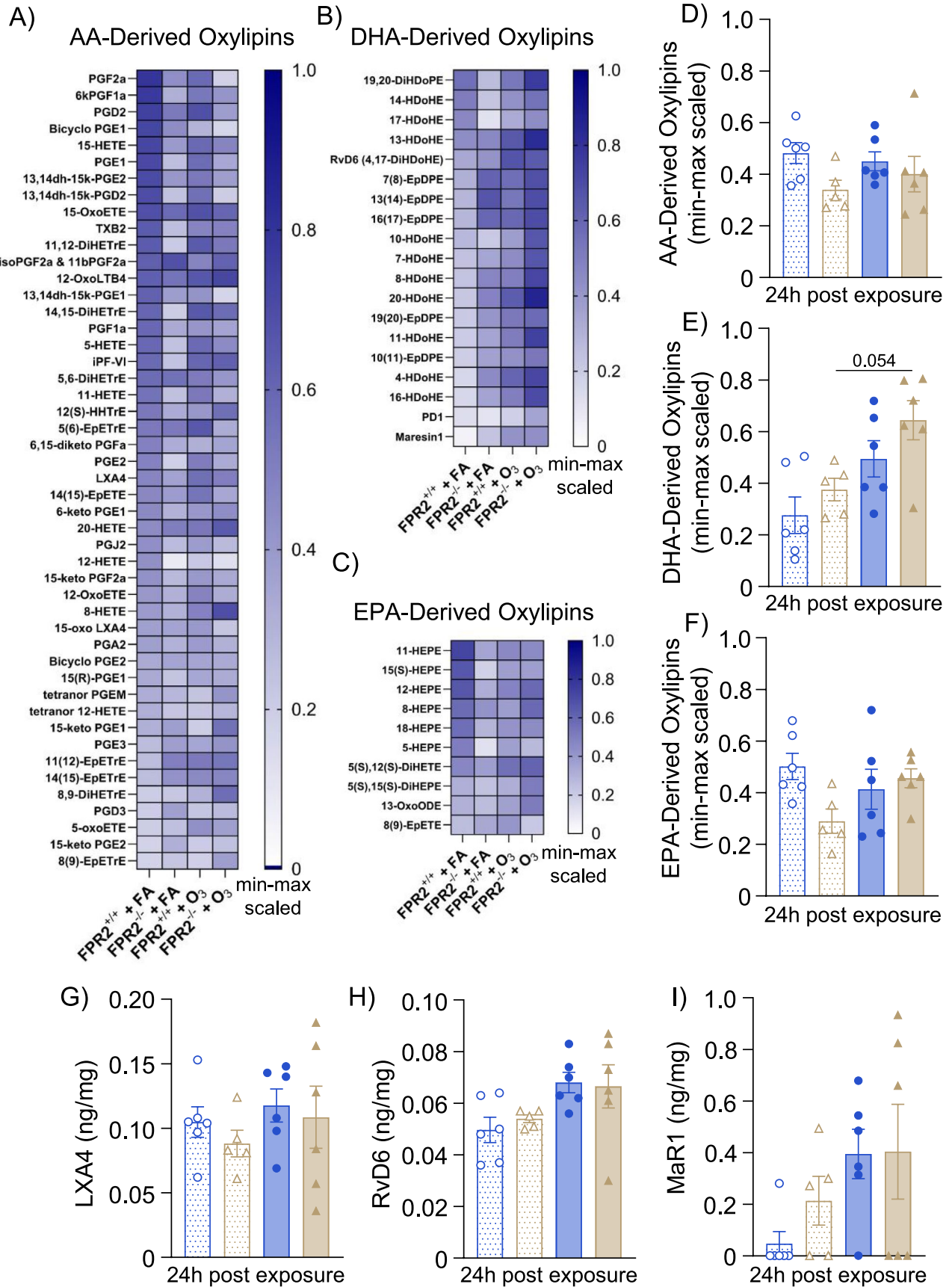


FIGURE 5 | Legend on next page.

FIGURE 5 | Loss of ALX/FPR2 does not influence pulmonary specialized pro-resolving mediators. ALX/FPR2 wild type (FPR2^{+/+}) or ALX/FPR2 knockout (FPR2^{-/-}) male mice 8–12 weeks old were exposed to filtered air (FA) or 1 ppm ozone (O₃) for 3 h and necropsied 24 h after the start of the exposure. Lung tissue was collected for LC-MS/MS analysis of oxylipins. Data were normalized by min-max scaling. Heatmap of normalized values for (A) arachidonic acid (AA)-derived oxylipins, (B) docosahexaenoic acid (DHA)-derived oxylipins, (C) eicosapentaenoic acid (EPA)-derived oxylipins. Average of normalized values for (D) AA-derived oxylipins, (E) DHA-derived oxylipins, (F) EPA-derived oxylipins. Tissue concentrations of selected specialized proresolving mediators (G) lipoxin A4 (LXA4), (H) resolvin D6 (RvD6), and (I) maresin 1 (MaR1). *n* = 5–6/group.

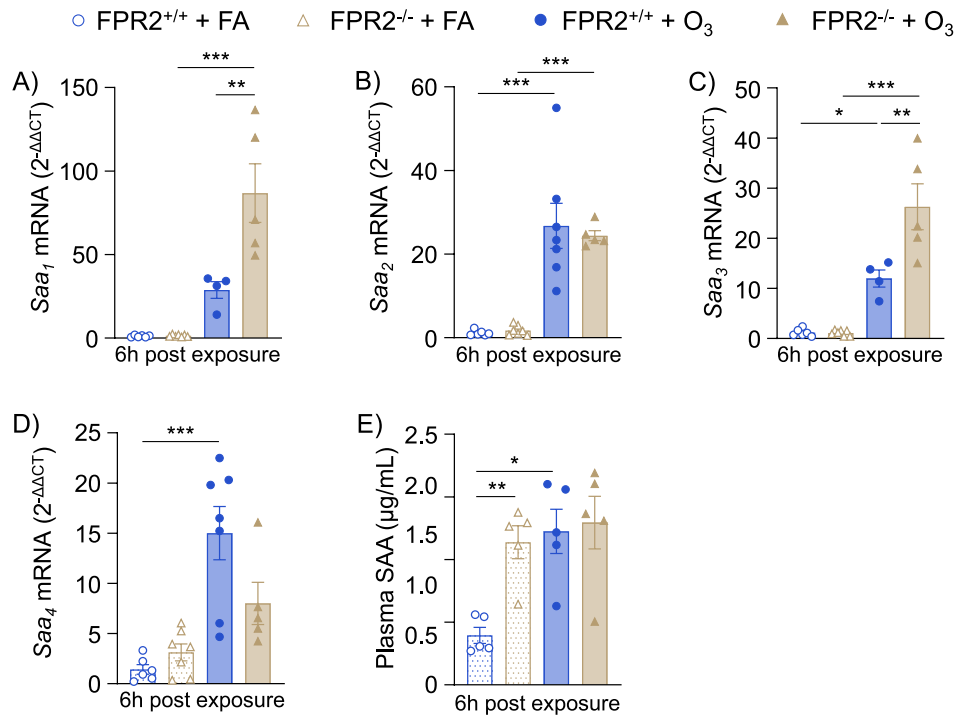


FIGURE 6 | Serum amyloid A expression and production is disrupted with loss of ALX/FPR2. ALX/FPR2 wild type (FPR2^{+/+}) or ALX/FPR2 knockout (FPR2^{-/-}) male mice 8–12 weeks old were exposed to filtered air (FA) or 1 ppm ozone (O₃) for 3 h and necropsied 6 h after the start of the exposure. Lung tissue was collected for real-time PCR of (A) *Saa₁*, (B) *Saa₂*, (C) *Saa₃*, (D) *Saa₄*. (E) Plasma was collected for ELISA analysis of total SAA. **p* < 0.05, ***p* < 0.01, ****p* < 0.001, *n* = 4–7/group.

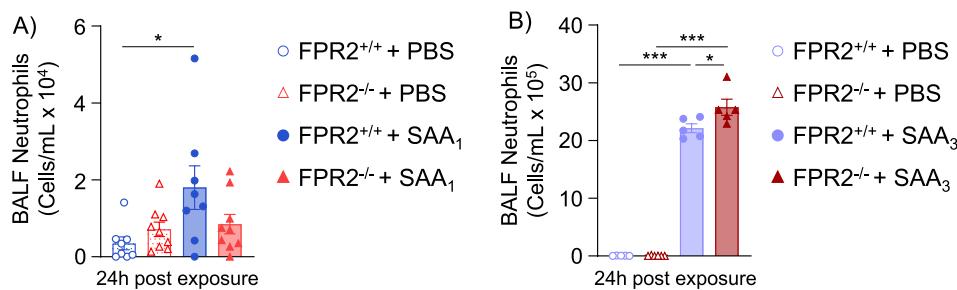


FIGURE 7 | Serum amyloid A contributes to neutrophil recruitment through ALX/FPR2. ALX/FPR2 wild type (FPR2^{+/+}) or ALX/FPR2 knockout (FPR2^{-/-}) male mice 8–12 weeks old were dosed with PBS or 10 μg/mouse SAA₁ by oropharyngeal aspiration (OA) and necropsied 24 h after dosing. (A) Bronchoalveolar lavage fluid (BALF) was collected for cellular differentials of neutrophils. (B) FPR2^{+/+} or FPR2^{-/-} male mice 8–12 weeks old were dosed with PBS or 10 μg/mouse SAA₃ by OA and necropsied 24 h after dosing. Bronchoalveolar lavage fluid (BALF) was collected for cellular differentials of neutrophils. **p* < 0.05, ***p* < 0.01, ****p* < 0.001, *n* = 5–6/group.

FPR2^{-/-} mice dosed with SAA₃ had increased BALF neutrophils, and neutrophils were significantly increased in FPR2^{-/-} mice compared to FPR2^{+/+} mice (Figure 7B). These data imply that SAA₁, but not SAA₃, signals through ALX/FPR2 to induce neutrophil recruitment to the lung.

4 | Discussion

The data presented here indicate that ALX/FPR2 is required to initiate neutrophil recruitment in the lungs following O₃ exposure. We identified that ALX/FPR2 is not required for the

pulmonary production of neutrophil-recruiting chemokines or SPMs. However, pulmonary and systemic SAA were significantly altered in mice lacking ALX/FPR2, suggesting a disruption in the ALX/FPR2–SAA signaling axis. Additionally, ALX/FPR2-deficient mice were insensitive to SAA₁-mediated lung neutrophil recruitment, indicating that SAA₁ requires ALX/FPR2 to recruit lung neutrophils. These findings reveal a novel role for SAA–ALX/FPR2 signaling during O₃-induced lung inflammation.

As a receptor for two SPM species, ALX/FPR2 has primarily been studied for its anti-inflammatory and/or proresolving roles [27]. However, there is also evidence for ALX/FPR2 signaling in proinflammatory pathways [28]. The present study focuses on the proinflammatory role of ALX/FPR2 as highlighted by disrupted neutrophil recruitment (Figure 2) and altered SAA production (Figure 6) in FPR2^{−/−} mice. SAA is a family of four proteins with similar functions (SAA_{1–4}) and is classically a biomarker of inflammation [25]. SAA₁ and SAA₂ have similar amino acid sequences in both mice and humans and are mostly produced in the liver during acute phase responses [41]. SAA₃ is also expressed in both mice and humans (although possibly as a pseudogene in humans as discussed later), mostly in nonhepatic cells such as epithelial and hematopoietic cells during the acute phase response [42]. SAA₄ is constitutively expressed and is generally considered not to be involved in the acute phase response [40]. The SAA proteins are generally grouped together when discussing the acute phase response, but our work and others' have indicated there are significant differences between these family members [43, 44]. For example, SAA₁/SAA₂ are downregulated while SAA₃ is upregulated during amyloidosis [43]. Furthermore, SAA₃ was reported to signal specifically through the TLR4/MD-2 pathway while SAA₁ favors signaling through FPR1 or ALX/FPR2 [44]. SAA₁ has been reported to induce neutrophil chemotaxis although this mechanism has not previously been defined during O₃ responses [45, 46]. Furthermore, there are several studies indicating “SAA” (subtype not specified) induces neutrophil recruitment [47–49] while, to the best of our knowledge, the neutrophil chemotactic ability of SAA₃ has only been observed by association [50]. In the context of O₃, previous studies have reported that *Saa*₁ and *Saa*₂ expression in liver tissue and total SAA protein in the blood are increased following rodent exposure [51]. In addition, similar to our results, *Saa*₃ was significantly increased in lung tissue of O₃ exposed mice [52]. Therefore, SAAs are present following O₃ exposure; however, it is unclear if a particular SAA family member is dominant in this response or if this is dependent on ALX/FPR2.

In this study, pulmonary expression of all *Saa* genes was increased after O₃ exposure. Interestingly, O₃-induced lung *Saa*₁ and *Saa*₃ expressions were higher in the FPR2^{−/−} mice compared to FPR2^{+/+} mice, while *Saa*₂ did not differ in FPR2^{−/−} mice compared to FPR2^{+/+} and *Saa*₄ did not increase after O₃ exposure in FPR2^{−/−} mice (Figure 6). This suggests ALX/FPR2 differentially influences SAA family members' transcription. SAA transcription is induced by pro-inflammatory cytokines such as IL-6, which binds the receptor gp130 to induce STAT3 transcription of SAA₁ [53]. SAA₁ transcription is also regulated by AP-2 and NF-κB [54]. In addition, IL-6 or IL-1β can synergistically enhance NF-κB interaction with the SAA₃ promoter [55, 56]. In this study, IL-6 and IL-1β were only statistically increased after

O₃ exposure in FPR2^{+/+} mice (Figure 4B). This suggests that the loss of ALX/FPR2 may have reduced cytokine signaling associated with *Saa*₁ and *Saa*₃ transcription. In the context of O₃, it is unclear how IL-6/IL-1β concentrations relate to SAA transcripts; however, the loss of ALX/FPR2 could disrupt temporal regulation of cytokine and/or SAA signaling. There are also potential feedback mechanisms that regulate SAA transcription [39]. It has been proposed that SAA leads to recruitment and enhanced survival of myeloid-derived suppressor cells (MDSCs) which downregulate IL-1β/IL-6 production and therefore inhibit further SAA transcription [39]. If the loss of ALX/FPR2 disrupts MDSC recruitment and prevents the downregulation of SAA, then this may account for the overexpression of *Saa*₁ and *Saa*₃ observed in FPR2^{−/−} mice (Figure 6A,C). Further research is needed to better understand how ALX/FPR2 regulates pulmonary SAA transcription and translation.

We also investigated how ALX/FPR2 influences how the lungs respond to increased SAA. Our findings show that OA administration of SAA₁ and SAA₃ resulted in differential neutrophil recruitment responses (Figure 7). SAA₃ induced a much more robust neutrophil response when compared to SAA₁, which may be attributed to differing inflammatory potentials of these SAA family members. Gutierrez et al. reported, in a metal oxide model of inflammation, that plasma SAA₃ levels were 1/100th or less the concentration of SAA₁ [57]. Therefore, lung cells may be more sensitive to SAA₃ than SAA₁. Interestingly, loss of ALX/FPR2 caused a decreased neutrophil response to SAA₁ but an increased neutrophil response to SAA₃. The SAA family of proteins has also been reported to bind receptors other than ALX/FPR2, including TLR4 [58]. Deguchi et al. reported that SAA₃ induces peritoneal macrophage migration dependent on TLR4 but independent of ALX/FPR2, while SAA₁ is known to induce cell migration through ALX/FPR2 [44, 59, 60]. SAA₃ signaling through TLR4 may explain why neutrophils were increased in FPR2^{−/−} mice dosed with SAA₃, whereas neutrophils were decreased in FPR2^{−/−} mice dosed with SAA₁.

In addition to reduced neutrophil recruitment following O₃ exposure, FPR2^{−/−} mice also had increased neutrophils compared to FPR2^{+/+} mice after FA exposure (Figure 2E). This baseline increase in neutrophil recruitment may be explained by FPR2^{−/−} mice also having increased plasma SAA compared to FPR2^{+/+} mice after FA exposure (Figure 6E). ALX/FPR2 is required for maintaining tissue homeostasis at steady state [61]. Therefore, it is possible that the loss of ALX/FPR2 disrupted homeostasis, resulting in baseline systemic inflammation that was undetected by our current methods but led to increased plasma SAA. Currently, it is unclear whether this affected the pulmonary inflammatory response to O₃. Future studies will be focused on whether this disruption of homeostasis diminished O₃-induced innate immune responses.

This work demonstrates that loss of ALX/FPR2 significantly alters the pulmonary immune response to O₃ exposure; however, there are several avenues for future investigation. While ALX/FPR2 is most highly expressed in myeloid cells, it is also expressed in lung epithelial cells, the brain, testes, and several other organs [22]. It is possible that the whole-body knockout disrupts other mechanisms in the body, and future investigation will explore inducible or cell type specific knockouts to more

precisely elucidate the role of ALX/FPR2 in the pulmonary immune response to O₃ exposure. There is also a question of the translatability of this research because of known species differences in SAA₃. In humans, SAA₃ is considered a pseudogene because of a single nucleotide insertion leading to a frame shift and early termination of transcription [62]. However, humans express SAA₁ and SAA₂ extrahepatically as well, including in monocytes and monocyte-derived macrophages [63–65]. Furthermore, this has recently become a subject of discussion because human SAA₃ was observed to be expressed as a fusion transcript with SAA₂ and appeared to contribute to inflammation in human cells [66]. Another limitation of this research is that these data focused exclusively on the immune response in males. Sex-based differences in the pulmonary immune responses to O₃ have been reported by our group and others [27, 67]. Future studies will evaluate if sex can influence the ALX/FPR2 dependent responses following O₃.

In conclusion, the present study describes the contribution of ALX/FPR2 and SAA during the pulmonary inflammatory response following O₃ exposure. The data presented here indicate that ALX/FPR2 mediates SAA-induced neutrophil recruitment. Ultimately, these findings reveal a novel mechanism of O₃-induced inflammation with implications for novel potential therapeutic targets.

Author Contributions

M.J.Y., R.M.T., R.V., S.R.S., and K.M.G. conceived and designed the research. M.J.Y., N.Z., T.N., K.D.-R., H.B.L., E.S., G.H., B.S., and R.I.C. performed the research and acquired the data. M.J.Y., S.H., R.M.T., R.V., S.R.S., and K.M.G. analyzed and interpreted the data. All authors were involved in drafting and revising the manuscript.

Acknowledgments

This study was supported in part by grants from the National Institutes of Health S10RR027926 and S10OD032292 to the Lipidomics Core Facility of Wayne State University. Authors were supported financially by the following: F31ES036102-02 (to M.J.Y.); R01ES031253 (S.H.); P30DK056350 (to S.R.S.); R01ES031378 (to K.M.G. and S.R.S.); R01ES034350 (to R.M.T.).

Conflicts of Interest

M.J.Y., S.H., R.M.T., S.R.S., and K.M.G. report receiving funding from the National Institutes of Health. S.R.S. reports receiving funding from Metagenics Incorporated and Organic Technologies for work related to PUFAs and SPMs. The authors declare no other conflicts of interest.

Data Availability Statement

All data provided within this manuscript will be uploaded to a publicly available database upon acceptance for publication.

References

1. GBD 2019 Risk Factors Collaborators, “Global Burden of 87 Risk Factors in 204 Countries and Territories, 1990–2019: A Systematic Analysis for the Global Burden of Disease Study 2019,” *Lancet* 396 (2020): 1223–1249.
2. P. A. Bromberg, “Mechanisms of the Acute Effects of Inhaled Ozone in Humans,” *Biochimica et Biophysica Acta* 1860 (2016): 2771–2781.

3. S. M. Holm and J. R. Balmes, “Systematic Review of Ozone Effects on Human Lung Function, 2013 Through 2020,” *Chest* 161 (2022): 190–201.
4. AQMD, S. C., “Historical Ozone Air Quality Trends,” 2022.
5. A. G. Ortiz, “Air Quality in Europe—2019 Report,” 2019, <https://www.eea.europa.eu/publications/air-quality-in-europe-2019>.
6. A. M. Vicedo-Cabrera, F. Sera, C. Liu, et al., “Short Term Association Between Ozone and Mortality: Global Two Stage Time Series Study in 406 Locations in 20 Countries,” *British Medical Journal* 368 (2020): m108, <https://doi.org/10.1136/bmj.m108>.
7. M. L. Bell, A. McDermott, S. L. Zeger, J. M. Samet, and F. Dominici, “Ozone and Short-Term Mortality in 95 US Urban Communities, 1987–2000,” *JAMA* 292 (2004): 2372–2378.
8. H. Gao, K. Wang, W. W. Au, W. Zhao, and Z. L. Xia, “A Systematic Review and Meta-Analysis of Short-Term Ambient Ozone Exposure and COPD Hospitalizations,” *International Journal of Environmental Research and Public Health* 17, no. 6 (2020): 2130, <https://doi.org/10.3390/ijerph17062130>.
9. J. I. Halonen, T. Lanki, T. Yli-Tuomi, M. Kulmala, P. Tiittanen, and J. Pekkanen, “Urban Air Pollution, and Asthma and COPD Hospital Emergency Room Visits,” *Thorax* 63 (2008): 635–641.
10. C. H. Wiegman, F. Li, B. Ryffel, D. Togbe, and K. F. Chung, “Oxidative Stress in Ozone-Induced Chronic Lung Inflammation and Emphysema: A Facet of Chronic Obstructive Pulmonary Disease,” *Frontiers in Immunology* 11 (2020): 1957.
11. S. C. Hu, A. Ben-Jebria, and J. S. Ultman, “Longitudinal Distribution of Ozone Absorption in the Lung: Effects of Respiratory Flow,” *Journal of Applied Physiology* 77, no. 2 (1994): 574–583, <https://doi.org/10.1152/jappl.1994.77.2.574>.
12. Z. Li, E. N. Potts-Kant, S. Garantziotis, W. M. Foster, and J. W. Hollingsworth, “Hyaluronan Signaling During Ozone-Induced Lung Injury Requires TLR4, MyD88, and TIRAP,” *PLoS One* 6 (2011): e27137.
13. P. M. Lepper, M. Triantafilou, L. A. O'Neill, et al., “Modulation of Toll-Like Receptor Signalling as a New Therapeutic Principle,” *Mediators of Inflammation* 2010 (2010): 705612.
14. P. N. Moynagh, “The NF-kappaB Pathway,” *Journal of Cell Science* 118, no. Pt 20 (2005): 4589–4592, <https://doi.org/10.1242/jcs.02579>.
15. K. Arsalane, P. Gosset, D. Vanhee, et al., “Ozone Stimulates Synthesis of Inflammatory Cytokines by Alveolar Macrophages In Vitro,” *American Journal of Respiratory Cell and Molecular Biology* 13 (1995): 60–68.
16. R. A. Johnston, J. P. Mizgerd, and S. A. Shore, “CXCR2 Is Essential for Maximal Neutrophil Recruitment and Methacholine Responsiveness After Ozone Exposure,” *American Journal of Physiology. Lung Cellular and Molecular Physiology* 288 (2005): L61–L67.
17. B. Kilburg-Basnyat, S. W. Reece, M. J. Crouch, et al., “Specialized Pro-Resolving Lipid Mediators Regulate Ozone-Induced Pulmonary and Systemic Inflammation,” *Toxicological Sciences* 163 (2018): 466–477.
18. A. Planaguma, S. Kazani, G. Marigowda, et al., “Airway Lipoxin A4 Generation and Lipoxin A4 Receptor Expression Are Decreased in Severe Asthma,” *American Journal of Respiratory and Critical Care Medicine* 178 (2008): 574–582.
19. A. P. Rogerio, O. Haworth, R. Croze, et al., “Resolvin D1 and Aspirin-Triggered Resolvin D1 Promote Resolution of Allergic Airways Responses,” *Journal of Immunology* 189 (2012): 1983–1991.
20. V. V. Horewicz, S. Crestani, R. de Sordi, E. Rezende, and J. Assreuy, “FPR2/ALX Activation Reverses LPS-Induced Vascular Hyporeactivity in Aorta and Increases Survival in a Pneumosepsis Model,” *European Journal of Pharmacology* 746 (2015): 267–273.

21. M. He, N. Cheng, W. W. Gao, et al., "Characterization of Quin-C1 for Its Anti-Inflammatory Property in a Mouse Model of Bleomycin-Induced Lung Injury," *Acta Pharmacologica Sinica* 32 (2011): 601–610.
22. M. G. Duvall, T. R. Bruggemann, and B. D. Levy, "Bronchoprotective Mechanisms for Specialized Pro-Resolving Mediators in the Resolution of Lung Inflammation," *Molecular Aspects of Medicine* 58 (2017): 44–56.
23. C. N. Serhan, C. B. Clish, J. Brannon, S. P. Colgan, N. Chiang, and K. Gronert, "Novel Functional Sets of Lipid-Derived Mediators With Anti-inflammatory Actions Generated From Omega-3 Fatty Acids via Cyclooxygenase 2-Nonsteroidal Antiinflammatory Drugs and Transcellular Processing," *Journal of Experimental Medicine* 192 (2000): 1197–1204.
24. C. N. Serhan, N. Chiang, J. Dalli, and B. D. Levy, "Lipid Mediators in the Resolution of Inflammation," *Cold Spring Harbor Perspectives in Biology* 7, no. 2 (2014): a016311, <https://doi.org/10.1101/cshperspect.a016311>.
25. S. Bozinovski, D. Anthony, G. P. Anderson, L. B. Irving, B. D. Levy, and R. Vlahos, "Treating Neutrophilic Inflammation in COPD by Targeting ALX/FPR2 Resolution Pathways," *Pharmacology & Therapeutics* 140 (2013): 280–289.
26. S. N. Cooray, T. Gobbetti, T. Montero-Melendez, et al., "Ligand-Specific Conformational Change of the G-Protein-Coupled Receptor ALX/FPR2 Determines Proresolving Functional Responses," *Proceedings of the National Academy of Sciences of the United States of America* 110, no. 45 (2013): 18232–18237, <https://doi.org/10.1073/pnas.1308253110>.
27. M. J. Yaeger, S. W. Reece, B. Kilburg-Basnyat, et al., "Sex Differences in Pulmonary Eicosanoids and Specialized pro-Resolving Mediators in Response to Ozone Exposure," *Toxicological Sciences* 183 (2021): 170–183.
28. S. M. Mooney, E. Billings, M. McNew, C. A. Munson, S. R. Shaikh, and S. M. Smith, "Behavioral Changes in FPR2/ALX and Chemr23 Receptor Knockout Mice Are Exacerbated by Prenatal Alcohol Exposure," *Frontiers in Neuroscience* 17 (2023): 1187220.
29. G. E. Hatch, R. Slade, L. P. Harris, et al., "Ozone Dose and Effect in Humans and Rats. A Comparison Using Oxygen-18 Labeling and Bronchoalveolar Lavage," *American Journal of Respiratory and Critical Care Medicine* 150 (1994): 676–683.
30. M. J. Wiester, J. S. Tepper, M. E. King, M. G. Menache, and D. L. Costa, "Comparative Study of Ozone (O₃) Uptake in Three Strains of Rats and in the Guinea Pig," *Toxicology and Applied Pharmacology* 96 (1988): 140–146.
31. R. M. Tighe, A. Birukova, M. J. Yaeger, S. W. Reece, and K. M. Gowdy, "Euthanasia- and Lavage-Mediated Effects on Bronchoalveolar Measures of Lung Injury and Inflammation," *American Journal of Respiratory Cell and Molecular Biology* 59 (2018): 257–266.
32. W. C. Lin, K. M. Gowdy, J. H. Madenspacher, et al., "Epithelial Membrane Protein 2 Governs Transepithelial Migration of Neutrophils Into the Airspace," *Journal of Clinical Investigation* 130 (2020): 157–170.
33. E. M. Sullivan, A. Fix, M. J. Crouch, et al., "Murine Diet-Induced Obesity Remodels Cardiac and Liver Mitochondrial Phospholipid Acyl Chains With Differential Effects on Respiratory Enzyme Activity," *Journal of Nutritional Biochemistry* 45 (2017): 94–103.
34. Y. R. Yu, E. G. O'Koren, D. F. Hotten, et al., "A Protocol for the Comprehensive Flow Cytometric Analysis of Immune Cells in Normal and Inflamed Murine Non-Lymphoid Tissues," *PLoS One* 11, no. 3 (2016): e0150606, <https://doi.org/10.1371/journal.pone.0150606>.
35. H. Henderi, "Comparison of Min-Max Normalization and Z-Score Normalization in the K-Nearest Neighbor (kNN) Algorithm to Test the Accuracy of Types of Breast Cancer," *IJIS: International Journal of Informatics and Information Systems* 4 (2021): 13–20.
36. P. V. Afonso, M. Janka-Junttila, Y. J. Lee, et al., "LTB4 Is a Signal-Relay Molecule During Neutrophil Chemotaxis," *Developmental Cell* 22 (2012): 1079–1091.
37. H. Wang, D. Anthony, S. Yatmaz, et al., "Aspirin-Triggered Resolvin D1 Reduces Pneumococcal Lung Infection and Inflammation in a Viral and Bacterial Coinfection Pneumonia Model," *Clinical Science (London, England)* 131 (2017): 2347–2362.
38. R. I. Sperling, "The Effects of Dietary n-3 Polyunsaturated Fatty Acids on Neutrophils," *Proceedings of the Nutrition Society* 57, no. 4 (1998): 527–534, <https://doi.org/10.1079/pns19980077>.
39. G. H. Sack, Jr., "Serum Amyloid A—A Review," *Molecular Medicine* 24 (2018): 46.
40. M. De Buck, M. Gouwy, J. M. Wang, et al., "Structure and Expression of Different Serum Amyloid A (SAA) Variants and Their Concentration-Dependent Functions During Host Insults," *Current Medicinal Chemistry* 23, no. 17 (2016): 1725–1755, <https://doi.org/10.2174/0929867323666160418114600>.
41. G. H. Sack, Jr., "Serum Amyloid A (SAA) Proteins," *Sub-Cellular Biochemistry* 94 (2020): 421–436.
42. G. Ramadori, J. D. Sipe, and H. R. Colten, "Expression and Regulation of the Murine Serum Amyloid A (SAA) Gene in Extrahepatic Sites," *Journal of Immunology* 135 (1985): 3645–3647.
43. H. Rokita, T. Shirahama, A. S. Cohen, R. L. Meek, E. P. Benditt, and J. D. Sipe, "Differential Expression of the Amyloid SAA 3 Gene in Liver and Peritoneal Macrophages of Mice Undergoing Dissimilar Inflammatory Episodes," *Journal of Immunology* 139 (1987): 3849–3853.
44. A. Deguchi, T. Tomita, T. Omori, et al., "Serum Amyloid A3 Binds MD-2 to Activate p38 and NF-kappaB Pathways in a MyD88-Dependent Manner," *Journal of Immunology* 191 (2013): 1856–1864.
45. M. De Buck, N. Berghmans, N. Portner, et al., "Serum Amyloid A1alpha Induces Paracrine IL-8/CXCL8 via TLR2 and Directly Synergizes With This Chemokine via CXCR2 and Formyl Peptide Receptor 2 to Recruit Neutrophils," *Journal of Leukocyte Biology* 98 (2015): 1049–1060.
46. M. De Buck, M. Gouwy, N. Berghmans, et al., "COOH-Terminal SAA1 Peptides Fail to Induce Chemokines but Synergize With CXCL8 and CCL3 to Recruit Leukocytes via FPR2," *Blood* 131 (2018): 439–449.
47. M. Kanther, S. Tomkovich, S. Xiaolun, et al., "Commensal Microbiota Stimulate Systemic Neutrophil Migration Through Induction of Serum Amyloid A," *Cellular Microbiology* 16, no. 7 (2014): 1053–1067, <https://doi.org/10.1111/cmi.12257>.
48. R. L. He, J. Zhou, C. Z. Hanson, J. Chen, N. Cheng, and R. D. Ye, "Serum Amyloid A Induces G-CSF Expression and Neutrophilia via Toll-Like Receptor 2," *Blood* 113 (2009): 429–437.
49. D. Anthony, H. J. Seow, M. Uddin, et al., "Serum Amyloid A Promotes Lung Neutrophilia by Increasing IL-17A Levels in the Mucosa and Gammadelta T Cells," *American Journal of Respiratory and Critical Care Medicine* 188 (2013): 179–186.
50. T. Dokoshi, L. J. Zhang, F. Li, et al., "Hyaluronan Degradation by Cemp Regulates Host Defense Against *Staphylococcus aureus* Skin Infection," *Cell Reports* 30 (2020): 61–68.e64.
51. M. A. Erickson, J. Jude, H. Zhao, et al., "Serum Amyloid A: An Ozone-Induced Circulating Factor With Potentially Important Functions in the Lung-Brain Axis," *FASEB Journal* 31 (2017): 3950–3965.
52. D. I. Kasahara, H. Y. Kim, J. A. Mathews, et al., "Pivotal Role of IL-6 in the Hyperinflammatory Responses to Subacute Ozone in Adiponectin-Deficient Mice," *American Journal of Physiology. Lung Cellular and Molecular Physiology* 306 (2014): L508–L520.
53. K. Hagihara, T. Nishikawa, Y. Sugamata, et al., "Essential Role of STAT3 in Cytokine-Driven NF-kappaB-Mediated Serum Amyloid A Gene Expression," *Genes to Cells* 10 (2005): 1051–1063.
54. Y. Ren and W. S. Liao, "Transcription Factor AP-2 Functions as a Repressor That Contributes to the Liver-Specific Expression of Serum Amyloid A1 Gene," *Journal of Biological Chemistry* 276, no. 21 (2001): 17770–17778, <https://doi.org/10.1074/jbc.M010307200>.

55. Z. Bing, J. H. Huang, and W. S. Liao, "NFkappa B Interacts With Serum Amyloid A3 Enhancer Factor to Synergistically Activate Mouse Serum Amyloid A3 Gene Transcription," *Journal of Biological Chemistry* 275, no. 41 (2000): 31616–31623, <https://doi.org/10.1074/jbc.M005378200>.
56. J. H. Huang and W. S. Liao, "Synergistic Induction of Mouse Serum Amyloid A3 Promoter by the Inflammatory Mediators IL-1 and IL-6," *Journal of Interferon & Cytokine Research* 19, no. 12 (1999): 1403–1411, <https://doi.org/10.1089/107999099312867>.
57. C. T. Gutierrez, C. Loizides, I. Hafez, et al., "Acute Phase Response Following Pulmonary Exposure to Soluble and Insoluble Metal Oxide Nanomaterials in Mice," *Particle and Fibre Toxicology* 20 (2023): 4.
58. R. D. Ye and L. Sun, "Emerging Functions of Serum Amyloid A in Inflammation," *Journal of Leukocyte Biology* 98 (2015): 923–929.
59. T. S. Liang, J. M. Wang, P. M. Murphy, and J. L. Gao, "Serum Amyloid A Is a Chemotactic Agonist at FPR2, a Low-Affinity N-Formylpeptide Receptor on Mouse Neutrophils," *Biochemical and Biophysical Research Communications* 270 (2000): 331–335.
60. S. Abouelasrar Salama, M. Gouwy, J. Van Damme, and S. Struyf, "Acute-Serum Amyloid A and A-SAA-Derived Peptides as Formyl Peptide Receptor (FPR) 2 Ligands," *Frontiers in Endocrinology* 14 (2023): 1119227.
61. M. Maciuszek, A. Cacace, E. Brennan, C. Godson, and T. M. Chapman, "Recent Advances in the Design and Development of Formyl Peptide Receptor 2 (FPR2/ALX) Agonists as Pro-Resolving Agents With Diverse Therapeutic Potential," *European Journal of Medicinal Chemistry* 213 (2021): 113167.
62. G. H. Sack, Jr., N. Zachara, N. Rosenblum, et al., "Serum Amyloid A1 (SAA1) Protein in Human Colostrum," *FEBS Open Bio* 8 (2018): 435–441.
63. C. Jumeau, F. Awad, E. Assrawi, et al., "Expression of SAA1, SAA2 and SAA4 Genes in Human Primary Monocytes and Monocyte-Derived Macrophages," *PLoS One* 14 (2019): e0217005.
64. C. Calero, E. Arellano, J. L. Lopez-Villalobos, V. Sanchez-Lopez, N. Moreno-Mata, and J. L. Lopez-Campos, "Differential Expression of C-Reactive Protein and Serum Amyloid A in Different Cell Types in the Lung Tissue of Chronic Obstructive Pulmonary Disease Patients," *BMC Pulmonary Medicine* 14 (2014): 95.
65. E. Arellano-Orden, C. Calero Acuna, V. Sanchez-Lopez, et al., "Cellular Mechanisms Involved in the Pathogenesis of Airway Remodeling in Chronic Lung Disease," *European Clinical Respiratory Journal* 9 (2022): 2097377.
66. T. Tomita, K. Ieguchi, T. Sawamura, and Y. Maru, "Human Serum Amyloid A3 (SAA3) Protein, Expressed as a Fusion Protein With SAA2, Binds the Oxidized Low Density Lipoprotein Receptor," *PLoS One* 10 (2015): e0118835.
67. N. Fuentes, A. Roy, V. Mishra, N. Cabello, and P. Silveyra, "Sex-Specific microRNA Expression Networks in an Acute Mouse Model of Ozone-Induced Lung Inflammation," *Biology of Sex Differences* 9 (2018): 18.

Supporting Information

Additional supporting information can be found online in the Supporting Information section.